G-quadruplex antibody attenuates human gastric cancer cell proliferation and promotes apoptosis through hTERT/telomerase pathway

Y.-Q. ZHANG¹, J.-H. PEI¹, S.-S. SHI², J. ZHENG¹, J.-M. WANG¹, X.-S. GUO³, G.-Y. CUI⁴, X.-Y. WANG⁵, H.-P. ZHANG⁶, W.-Q. HU⁶

Abstract. – OBJECTIVE: To investigate the expression of G-quadruplex antibody BG4 in human gastric cancer AGS cells and assess its functions in attenuating proliferation and promoting apoptosis in gastric cancer.

MATERIALS AND METHODS: BG4 high-expression gastric cancer AGS cell line was established by pEGFP-N1-BG4 transient transfection. AGS cells transfected with pEGFP-N1 plasmids were included into the pEGFP-N1 group and those not transfected with plasmids were included into the negative control group. Cell counting kit-8 (CCK8) assay was performed to examine the AGS cell proliferation ability, while flow cytometry was used to detect the cell cycle distribution and cell apoptosis. Cell migration was measured using Transwell migration and wound healing assay. Then the expression levels of cell apoptosis associated factors were determined. The mRNA and protein expressions of human telomerase reverse transcriptase (hTERT), B-cell lymphoma 2 (Bcl-2), Bcl-2 associated X (Bax) were examined with real-time quantitative polymerase chain reaction (PCR) and Western blotting, respectively.

RESULTS: The results revealed that pEGFP-N1-BG4 group exhibited reduced proliferation and migration, induction of apoptosis. hTERT and BcI-2 mRNA and protein levels in pEGFP-N1-BG4 group were down-regulated compared with those in the pEGFP-N1 group and control group, but there were no significant differences in Bax mRNA and protein levels compared with those in the pEGFP-N1 group and control group.

CONCLUSIONS: We showed that the expression of BG4 in the gastric cancer cell line AGS in-

hibits cell proliferation and promotes apoptosis though inducing telomere to form G-quadruplex structure and attenuating telomerase activity, thus resulting in reduced expression of hTERT and Bcl-2.

Key Words:

Gastric cancer, Antibody, G-quadruplex, Proliferation, Apoptosis.

Introduction

Gastric cancer (GC) is one of the most common malignancies in the digestive system seriously threatening human health^{1, 2}. World cancer statistics show that stomach cancer is the third leading cause of cancer deaths in the world^{3, 4}. The incidence and mortality of GC rank second among most common malignant tumors in China⁵. Despite of improvements in the surveillance and treatment of GC, it remains a devastating disease. Therefore, it is important to explore the pathogenesis of GC and find effective treatments for this disease.

G-quadruplexes (also known as G-tetrads or G4) are nucleic acid secondary structures that form within guanine-rich sequences. These higher-order structures contain arranged G-tetrads connected by Hoogsteen hydrogen bonds and are stabilized by monovalent cations. It is proposed that G-quadruplex nucleic acids play a role in a number of fundamental biological processes including apoptosis,

¹Department of Biochemistry, Changzhi Medical College, Changzhi, Shanxi, Changzhi, China ²Department of Nephrology, Heji Hospital of Changzhi Medical College, Changzhi, Shanxi, Changzhi, China

³Department of Physiological, Changzhi Medical College, Changzhi, Shanxi, Changzhi, China ⁴Department of Microbiology, Changzhi Medical College, Changzhi, Shanxi, Changzhi, China ⁵First clinical department of Changzhi Medical College, Changzhi, Shanxi, Changzhi, China ⁶Department of general surgery, Heji Hospital of Changzhi Medical College, Changzhi, Shanxi, Changzhi, China

gene transcription and gene expression. Many putative G-quadruplex sequences are located in the promoters of oncogenes. In addition, human telomeres are proven to have potential therapeutic mechanisms and to be validated as targeting sites for drugs. Studies have demonstrated that telomerase, a complex formed by protein and RNA, has reverse transcriptase activity for the regulation of tumor proliferation and apoptosis^{6, 7}. The guanine-quadruplexes^{8, 9} are capable of forming a four-stranded structure in telomere, which impairs the functions of telomerase by repressing the replication of telomere¹⁰⁻¹². This eventually affects cell proliferation, differentiation and senility. In addition, the promoter regions¹³⁻¹⁵ of several cancer genes also can form G4 structure, and then influence its expression¹⁶⁻¹⁸.

Owing to the high affinity of G-quadruplex antibody BG4 with the G-quadruplex¹⁹ and abundant TG sequences in telomere region, BG4 can be used as a stabilizer for G4 interacting with the G-quadruplex in telomere and may serve as an inhibitor of telomerase (Figure 1). Studies have demonstrated that BG4 was employed to visualize DNA G-quadruplex structures in human cells^{20,21}. Biffi et al²² used BG4 antibody to detect a series of paraffin-embedded cancer and cancer-adjacent tissues by tissue microarray method. They found that the formation of G-quadruplexes was increased obviously in cancer than in the normal tissue in human GC and liver cancer, suggesting that the formation of G-quadruplexes may be a characteristic marker of GC. However, the function and mechanism of BG4 expression in GC are still unclear.

In order to better understand the function of BG4 protein, the pEGFP-N1-BG4 eukaryotic expression vector was constructed and then transfected into AGS cells by Lipofectamine 2000. The BG4 expression in AGS cells was verified by Western blotting analysis. The function of BG4 was determined by detecting cell proliferation, cell cycle, apoptosis and possible signal transduction molecules. The results demonstrated that BG4 displayed an inhibition effect for AGS cells. BG4 could suppress proliferation, induce cell apoptosis and arrest cell cycle in AGS cells through down-regulating hTERT and Bcl-2 expression *in vitro*.

Materials and Methods

Construction of pEGFP-N1-BG4 Expression Plasmid

Primer sequence: *Sac*I tailed forward: 5'-GGAGCTCATGGCCGAGGTGCAGCTG-3'; *Pst*I tailed reverse: 5'-CTGCTGCAGCTTGT-CATCGTCATCCTTGTAATC-3' (restriction sites were underlined), which were named as BG4-F and BG4-R, respectively. The length of the amplification segment was 877 bp. There are 6×Histidine tags and the 3×FLAG tags in BG4 protein. The whole sequence of BG4 was in the early stage of our study. There were a total of 50 μL reaction systems containing 36.5 μL ddH₂O, 0.5 μL Ex Taq (5 U/μL), 5 μL 10 ×polymerase chain reaction (PCR) buffer, 5 μL dNTP, 1 μL

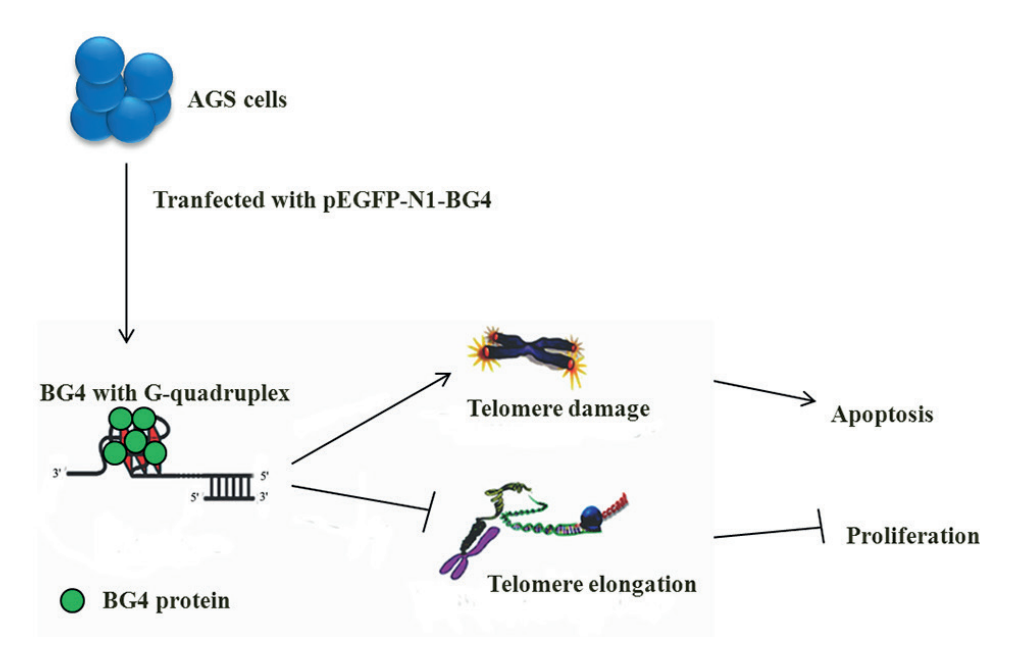


Figure 1. BG4, as a stabilizer for G4, interacts with the G-quadruplex in telomere and may serve as an inhibitor of telomerase.

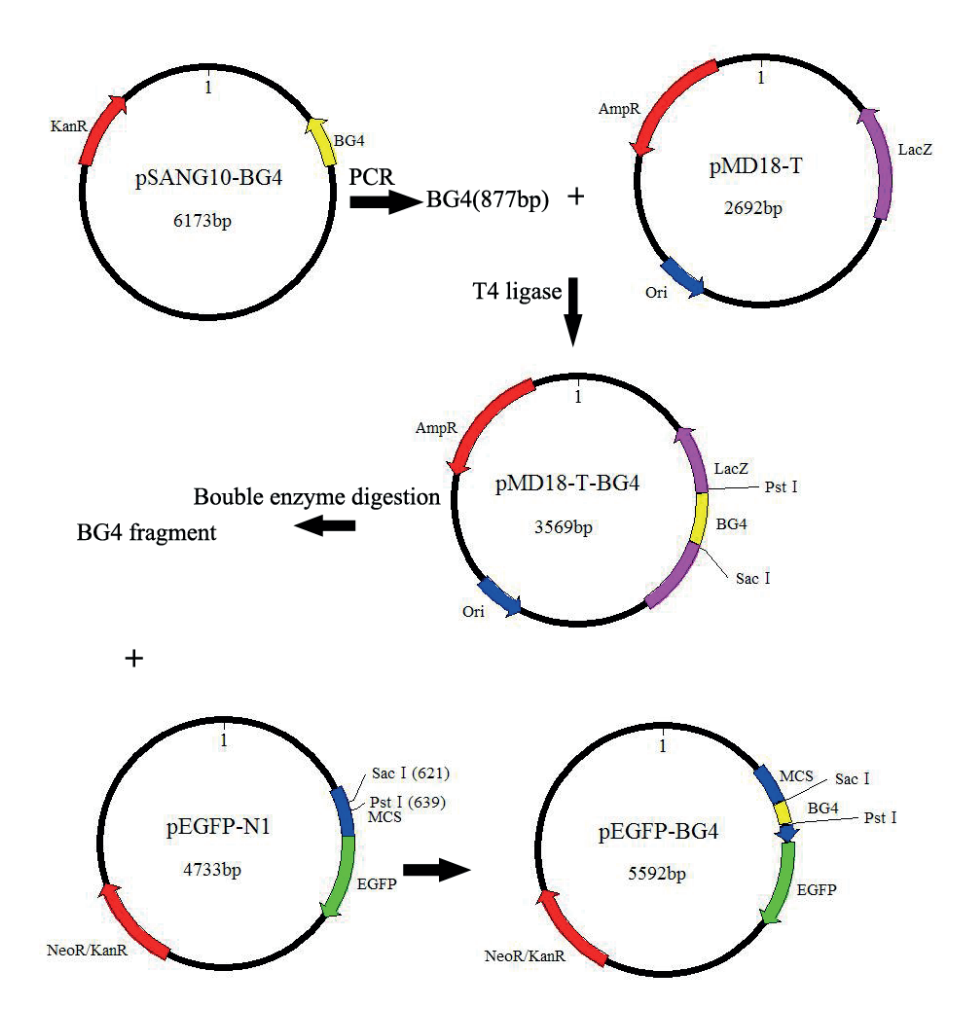


Figure 2. Construction of pEGFP-N1-BG4 expression plasmid.

BG4-F (10 μmol/L), 1 μL BG4-R (10 μmol/L) and 1 µL pSANG10-BG4 DNA. Procedure used in this study was as follows: pre-denaturation at 94°C for 10 min and 30 cycles of denaturation at 94°C for 30 s, annealing at 58°C for 30 s, and an extension at 72°C for 60 s, followed by 5 min of final extension at 72°C. The final PCR products were separated by electrophoresis using 1.5% agarose gel for 45 minutes under a constant voltage of 100 v. Then pictures were recorded. The target fragment was purified using Mini BEST Agarose Gel DNA Extraction Kit. The purified target fragments were ligated into the plasmid pMD18-T and then transformed into competent E. coli DH5a cells. Recombinant plasmid was extracted from bacterial colonies, and 1.0 µL plasmid solution was subjected to agarose gel electrophoresis to confirm the presence of the correct sequence of BG4. The recombinant plasmid that had been confirmed to contain the correct sequence of BG4

and the vector pEGFP-N1 were digested by *SacI* and *PstI*, respectively. The target fragments were isolated and ligated using T4 DNA ligase, and subsequently a second recombinant plasmid was constructed. The second recombinant plasmid was transformed into competent E. coli DH5α cells and then extracted by DNA purification kit. The resulting recombinant eukaryotic expression vector was named pEGFP-N1-BG4. The vector was digested using SacI and PstI and then evaluated by agarose gel electrophoresis. The recombinant plasmid was further sequenced to confirm its sequence (Figure 2).

Cell Culture and Intervention

The human GC AGS cells were obtained from the Institute of Biochemistry and Cell Biology, Chinese Academy of Sciences (Shanghai, China). Cells were maintained in Roswell Park Memorial Institute (RPMI)-1640 (01-100-1A, BI, Kibbutz Beit Haemek, Israel) medium with 10% fetal bovine serum (FBS) (04-001-1A, BI, Kibbutz Beit Haemek, Israel) and 100 U/mL penicillin plus 0.1 μg/mL streptomycin in a humidified incubator with 95% humidity and 5% CO₂ at 37°C.

AGS cells (1×10⁶cells/well) were cultured in RPMI-1640 medium in six-well plates with 10% FBS for 24h, and then they were divided into three groups: control, pEGFP-N1 and pEGFP-N1-BG4. After the medium was removed and replaced with serum free and antibiotic free RPMI-1640 medium for 6h before transfection, the complexes of plasmid and liposome were prepared according to recommended preparation methods of Lipofectamine TM2000 Reagent kit (Invitrogen, Carlsbad, CA, USA).

Cell Proliferation Assay

The effect of BG4 on cell proliferation of AGS cells was evaluated using WST tetrazolium salt (Dojindo, Japan) according to the manufacturer's instructions. AGS cells were plated into 96-well plates at 10³cells/well in triplicate in 100 μL of culture medium and allowed to adhere overnight. The three groups were incubated for 1, 2, 3, and 4 day, respectively. Each well received 10 μL of cell counting kit-8 solution (R&D Systems, Minneapolis, MN, USA) and incubated for 4 h. The absorbance was detected at 450 nm using a microplate reader (Thermo Fisher, Waltham, MA, USA) and expressed in optical density (OD) units. The experiment was performed in triplicate.

Cell Cycles and Apoptosis Assay

Forty-eight hours after transfection, cells were collected, washed with phosphate-buffered saline (PBS), fixed with 70% (v/v) ethanol (Sigma-Aldrich, St. Louis, MO, USA) at 4°C overnight, and centrifuged at 1,000 rpm/min for 5 min. Then ethanol was removed, and cells were stained with propidium iodide (PI). Cell cycle analysis was performed using a flow cytometer (BD, Franklin Lakes, NJ, USA). The effect of BG4 on cell apoptosis of AGS cells was investigated using Annexin V-APC Apoptosis Analysis Kit by flow cytometry (FACSort, BD, Franklin Lakes, NJ, USA) according to the manufacturer's instructions. Cells were harvested at 48 h after transfection and rinsed three times with cold PBS, and then 5 µL Annexin V-APC and 5 μL 7-aminoactinomycin (7-AAD) were added to the cells, respectively. After 15 min of incubation in the dark at room temperature and about 500 µL binding buffer was added, apoptosis was

evaluated by flow cytometry. Three independent experiments were done. Every sample was detected for three times.

Wound Healing Assay

AGS (5×10⁵ cells/well) were seeded in 6-well plates and then transiently transfected with pEG-FP-N1 and pEGFP-N1-BG4. When cells had grown 90% confluent, scratches were made to the monolayer surfaces of cells with sterile 200-µl pipette tips. After rinsing with PBS for 3 times, dead cells were removed, and the remaining cells were cultured in serum-free medium to eliminate the influence of cell proliferation. Micrographs were captured for each sample at 0 and 24 h. The relative migration rate was calculated using Image J software as follows: Relative migration rate = (gap between the edges at 0 h - gap between the edges at 24 h) / gap between the edges at 0 h.

Transwell Migration Assay

To assess invasion ability, 24-well Transwell chambers with an 8-µm pore size polycarbonate membrane were used (Corning Incorporated, Corning, NY, USA). The filters were precoated with 10 µg of Matrigel (BD, Franklin Lakes, NJ, USA). Then the chambers were inserted into a 24-well plate. Three groups of cells were suspended in serum-free culture media and added to upper chambers, respectively. After 24 h of incubation at 37 °C, cells inside the upper chamber were removed with cotton swabs, whereas cells on the lower membrane surface were fixed with 4% paraformaldehyde and then stained with 0.5% Crystal violet solution. Six randomly selected fields were counted in each well. Our preliminary experiments demonstrated that 10% FBS concentration is optimal for observing cell migration. Therefore, RPMI-1640 with 10% FBS was added into the lower chamber of each well, and the cells were incubated for 12 h. The medium and non-migrated cells in the upper chamber were removed gently with a cotton swab, whereas the migrated cells in the lower chamber were fixed with paraformaldehyde (4%) and stained with crystal violet. Images were captured at a magnification of 50 folds. Cells in 6 different fields were counted.

Real-Time Reverse Transcription and Polymerase Chain Reaction (RT-PCR) Analysis

Total ribonucleic acids (RNAs) of three groups were isolated from AGS cells using the RNAiso Plus (TaKaRa, Otsu, Shiga, Japan). The value

of ${\rm OD_{260}/\ OD_{280}}$ for RNA located in 1.9-2.1 was qualified. cDNA was synthesized using the Prime Script[™] RT-PCR Kit (TaKaRa, Otsu, Shiga, Japan) according to the manufacture's instruction. 2 μL cDNAs were served as a template to be amplified by Real-time PCR using SYBR® Premix Ex TaqTM II (TaKaRa, Otsu, Shiga, Japan) using the conditions as the manufacture instructed. The human β -actin gene was served as a control gene. The relative mRNA expressions of hTERT, Bcl-2, Bax were analyzed by real-time PCR using the IQTM5 System (Bio-Rad, Hercules, CA, USA). The primers were synthesized by ShengGong Co, Ltd and the sequences were displayed as follow: hTERT forward 5'-GGAGGCTCGTGGAGACCATC3', reverse 5'-CATTTGCCAGTAGCGCTGGG3'; Bcl-2 sense: 5'-CCTCCAGGTAGGCCCGTTTT-3', anti-sense: 5'-GGGCCTCTGTTCCTTCCCTC-3'; Bax sense: 5'-CCCAGAGGCGGGGTTTCA-3', anti-sense: 5'-GGAAAAAGACCTCTCGGGGGG-3'; β-actin sense: 5'-CCTGGCACCAGCACAAT-3', 5'-GGGCCGGACTCGTCATAC-3'. Relative mRNA expression was calculated with the $2^{-\Delta\Delta Ct}$ method. Every sample was detected for three times.

Protein Isolation and Western Blotting

Three groups of cells were and lysed with radioimmunoprecipitation assay (RIPA) lysis buffer, and the supernatant wascentrifuged (10000 g, 20 min) and separated. 12% sodium dodecyl sulphate-polyacrylamide gel electrophoresis (SDS-PAGE) was used to separate lysated proteins, which were then transferred to polyvinylidene difluoride (PVDF) membrane. PVDF membrane containing total proteins was blocking with 5% skimmed milk for 2 h, hTERT (sc-7212, Santa Cruz Biotechnology, Santa Cruz, CA, USA) (1:1000), Bcl-2 (sc-7382, Santa Cruz Biotechnology, Santa Cruz, CA, USA) (1:1000), Bax (sc-20067, Santa Cruz Biotechnology, Santa Cruz, CA, USA) (1:1000) and β-actin (sc-4778, Santa Cruz Biotechnology, Santa Cruz, CA, USA) (1:5000) antibodies were applied to detected the protein expression, respectively. Anti-FLAG-tag antibody was used for identifying BG4 expression. Secondary horseradish peroxidase (HRP)-conjugated goat anti-rabbit or anti-mouse antibody was used at a 1:5000 dilution and developed by the ECL Reagent (Millipore, Billerica, MA, USA).

Statistical Analysis

Measurement data were presented as (Mean ± SD). Statistical Product and Service Solu-

tions (SPSS) 22.0 (SPSS Inc., Armonk, NY, USA) was used for two-tailed Student-t test and ANOVA, and Least Significant Difference (LSD) was employed as its Post Hoc Test. p<0.05 represented that the difference was statistically significant.

Results

Construction of pEGFP-N1-BG4 Vector

The results confirmed that the construction of the pEGFP-N1-BG4 (5592 bp) eukaryotic expression plasmid was successful (Figure 3A). After double enzyme digestion, a 877 bp BG4 segment and a 4715 bp vector fragment were observed in the pEGFP-N1-BG4 group via electrophoresis, while only a 4.7 kb vector fragment was the same as the pEGFP-N1. The sequencing result is shown in Figure 3B. The protein of BG4 was expressed in pEGFP-N1-BG4 transfected AGS cells. The molecular weight of BG4 protein is 30-35 kDa and EGFP protein is 27 kDa. The molecular weight of fusion protein was 57-62 kDa. The target protein is 48-63 kDa and consistent with the theoretical size (Figure 3C).

Cell Apoptosis Assay

An apoptosis assay was performed after transfection with pEGFP-N1 and pEGFP-N1-BG4. The apoptotic rate was (2.39±0.04)% in the negative control group and (2.42±0.12)% in the pEGFP-N1 group, and after transfection with pEGFP-N1-BG4, the apoptotic rate was increased to (8.44±0.17)% (Figure 4A-B). These results demonstrated that pEGFP-N1-BG4 group induced apoptosis of AGS cells.

Cell Proliferation Assay

The CCK8 assay results illustrated that the cell proliferation in pEGFP-N1-BG4 group was obviously inhibited compared with that in other groups (**p<0.05). The pEGFP-N1 group and the NC group had no significant differences in the cellular growth at different time points (*p>0.05). The results indicated that the BG4 protein could inhibit the proliferation of AGS cells (Figure 4A-B).

pEGFP-N1-BG4 Arrested AGS Cells Cycle

Compared with NC group and pEGFP-N1 group, AGS cells could be effectively arrested at G_0/G_1 phase in pEGFP-N1-BG4 group, and cells were inhibited to run into S phase. Additional-

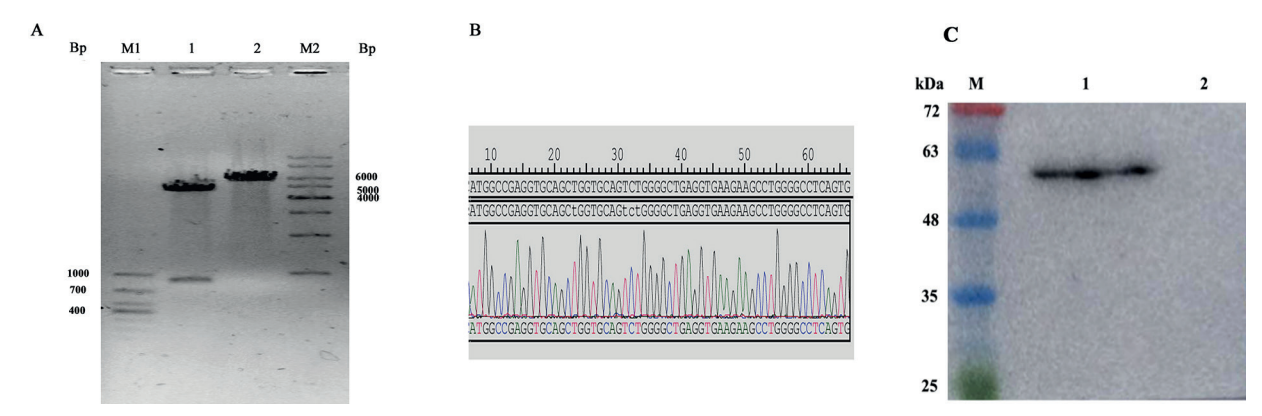


Figure 3. Identification of recombinant pEGFP-N1-BG4 plasmid. *A*, M1, M2: DL1000 DNA Ladder and 1 kb DNA Ladder. 1: pEGFP-N1-BG4 plasmid is digested with *Sac* I and *Pst* I enzyme (877bp for small fragment, 4715 bp for large fragment), and 2: pEGFP-N1-BG4 plasmid is digested with *Pst* I enzyme (5592bp). *B*, Sequencing results of pEGFP-N1-BG4 recombinant plasmid (partial). *C*, M: Standard molecular weight protein marker. 1: Cell lysates of AGS protein transfected with pEGFP-N1-BG4 vector, and 2: Cell lysates of AGS protein transfected with pEGFP-N1 vector.

ly, the percentage of apoptotic cells was also increased after they were transfected with pEGFP-N1-BG4 (Figure 5). The detailed data are shown in Table I.

Wound-Healing Assay

The migration capability of GCcells after transfection was assessed *via in-vitro* scratch assay. Figure 6 presents that the migration rate is (0.2640±0.002) in the negative control group, (0.2717±0.001) in cells transfected with pEG-FP-N101, and (0.077±0.002) in cells transfected with pEGFP-N1-BG4. Wound-healing assay revealed that transfection with pEGFP-N1-BG4 significantly inhibited wound healing compared with negative control group and pEGFP-N1 group (Figure 6, **p*<0.05).

pEGFP-N1-BG4 Group Inhibited Invasion Abilities of AGS Cells

Transwell invasion assay was adopted to explore the effect of BG4 on AGS cell invasion. the number of cells that passed through the Matrigel-coated membrane into the lower chamber

significantly inhibited in the pEGFP-N1-BG4 group in comparison with pEGFP-N1 group and negative control group (Figure 7, *p<0.05), suggesting that BG4 inhibits the invasion ability of AGS cells

pEGFP-N1-BG4 regulated the expression of hTERT, Bcl-2 and Bax in AGS cells

According to the results shown above, we knew that pEGFP-N1-BG4 group could suppress cell growth. To investigate the possible molecular mechanisms, we detected the mRNA and protein levels of hTERT, which is the key component that determines the telomerase activity, and Bcl-2 and Bax, which are two classic genes in cell growth regulation, by qPCR and western-blot. Figure 8 displays both mRNA and protein levels of hTERT are down-regulated in pEGFP-N1-BG4 group compared with those in NC group and pEGFP-N1 group (*p<0.05). Meanwhile, the expression level of Bcl-2 was also down-regulated in pEGFP-N1-BG4 group. However, there were no significant differences in the mRNA and protein levels of Bax among three groups (Figure 8).

Table I. Cell cycles and apoptosis in different groups.

	Apoptosis (%)			
Cell cycles	G _o /G ₁ phase (%)	S phase (%)	G2/M phase (%)	Apoptosis (%)
NC group pEGFP-N1 group pEGFP-N1-BG4 group	42.59±1.10 41.98±1.37 54.99±1.01	43.90±0.96 44.65±0.82 29.65±1.87	13.51±1.16 14.91±1.08 15.37±1.56	2.39±0.08 2.42±0.19 8.44±0.17

^{*}p<0.05 vs. NC group and pEGFP-N1 group

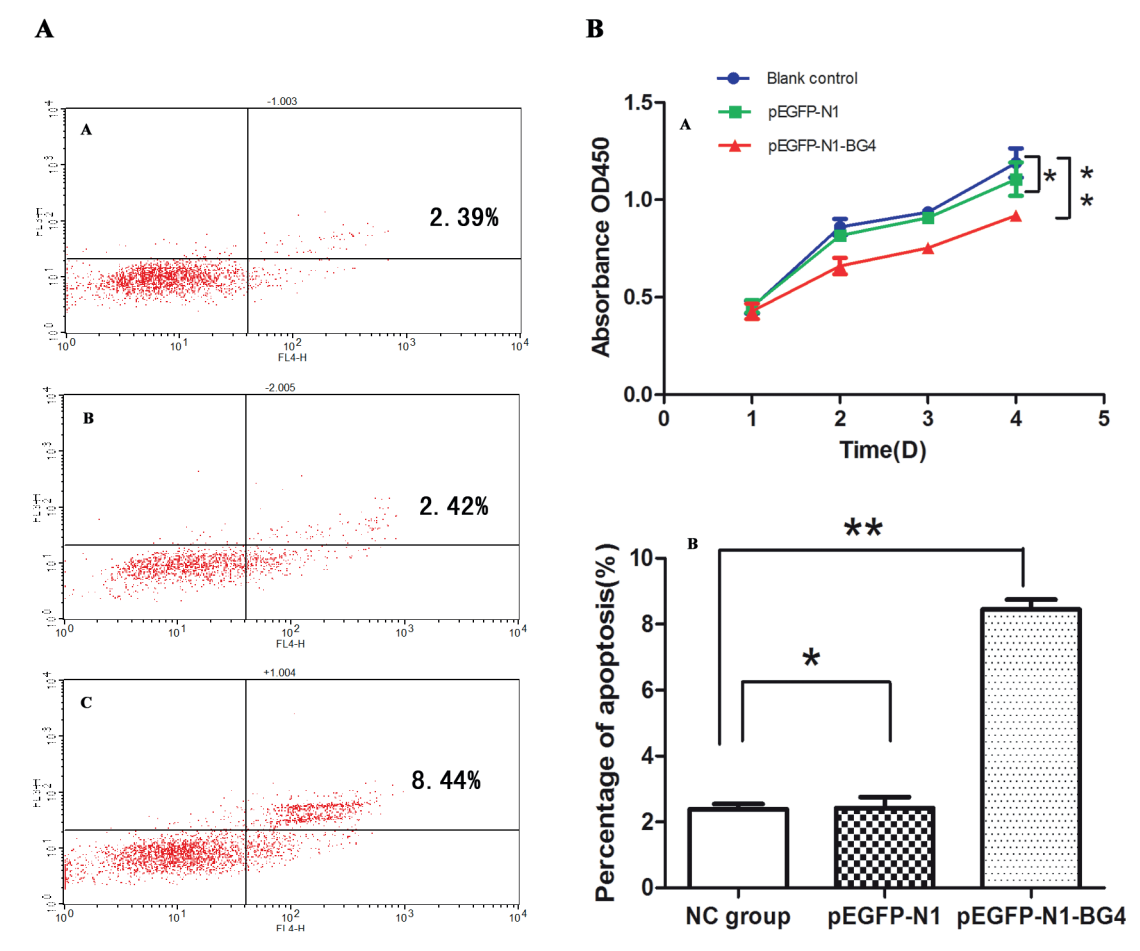


Figure 4. Apoptosis and cell viability analysis of AGS cells after transfection. *A-B*, The cell apoptotic rate of pEGFP-N1-BG4 group is higher than those of pEGFP-N1 group and NC group. The cell proliferation in pEGFP-N1-BG4 group is inhibited compared with those in pEGFP-N1 group and NC group, respectively. All data are analyzed using 2-tailed Student's *t*-tests. Error bars, **p*> 0.05, ** *p*<0.05.

Discussion

Telomeres are formed by telomere binding protein and DNA repetitive sequences that are rich in guanines²³. Located in 3'-end of the chromosomes, telomeres prevent DNA from degradation

and confluence in eukaryotic cells. This prevention effect will gradually lose with cell division. Fortunately, telomerases can maintain the length of telomeres, keeping the DNA stably²⁴. Telomerases are overexpressed in many human malignant tumors²⁵, but rare in normal tissues. Therefore,

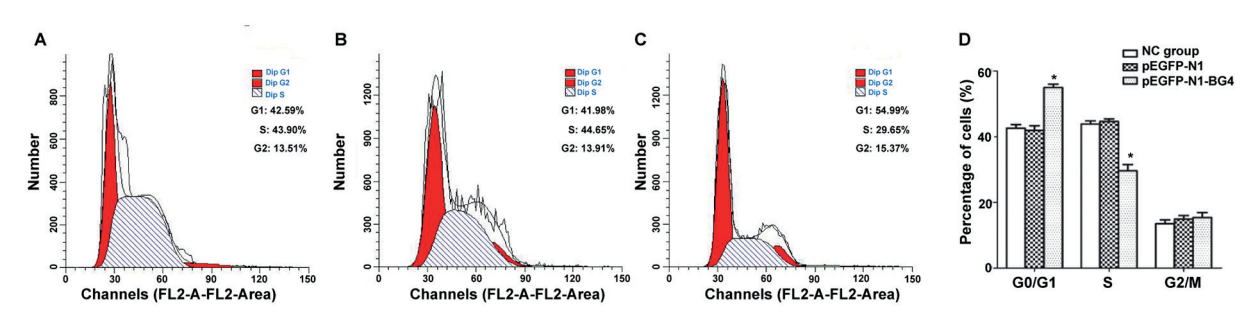


Figure 5. pEGFP-N1-BG4 arrests cell cycle. **A,** pEGFP-N1-BG4 arrests cells in G_0/G_1 phase and reduces the S phase's cell percentage. *p<0.05.vs. NC group and pEGFP-N1 group.

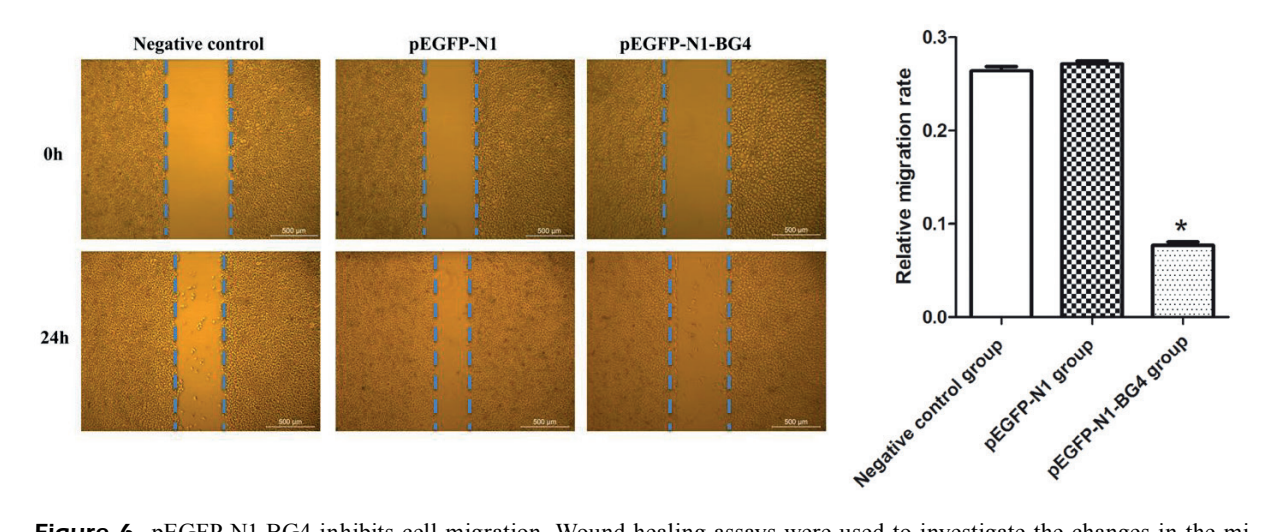


Figure 6. pEGFP-N1-BG4 inhibits cell migration. Wound healing assays were used to investigate the changes in the migratory ability of GC cells. The mean values and SD are calculated from triplicates of a representative experiment. *p<0.05.

they are commonly regarded as tumor biomarkers for prognostic assessment. Inhibitors of telomerases were designed for targeting different structures and components²⁶. G-quadruplex is composed of several guanine residues from telomere DNA, and its structural stabilizer has become a new type of telomerase inhibitor. Telomerases replicate only when combined with catenulate telomeres. If some substances promote the formation of G-quadruplex or stabilize the structure of G-quadruplex, they can hinder the uncoiled progression of telomeres²⁷, thereby suppressing the function of telomerases through impair their combination of telomeres²⁸. The structural stabilizers of G-quadruplex are more specific for tumor cells, so they can increase the accuracy of tumor targeting treatments, and reduce side-effects of chemotherapy²⁹.

In the present study, the biological function and the underlying mechanism of BG4 in AGS cells were preliminarily identified. The results demonstrated that pEGFP-N1-BG4 successfully inhibited the extension of telomeres mediated by telomerases and promoted the formation of G-quadruplex in AGS cells. pEG-FP-N1-BG4 could induce both telomere shortening and apoptosis in AGS cell line through changing the sheer force of hTERT. Similarly, we also found that pEGFP-N1-BG4 could markedly down-regulate the expression of hTERT in AGS cells. The formation of G-quadruplex could inhibit DNA replications and arrest cell cycles. In our study, compared with those in NC group and pEGFP-N1 group, the percentage of G₀/G₁-phase AGS cells was significantly increased in pEGFP-N1-BG4 group, while

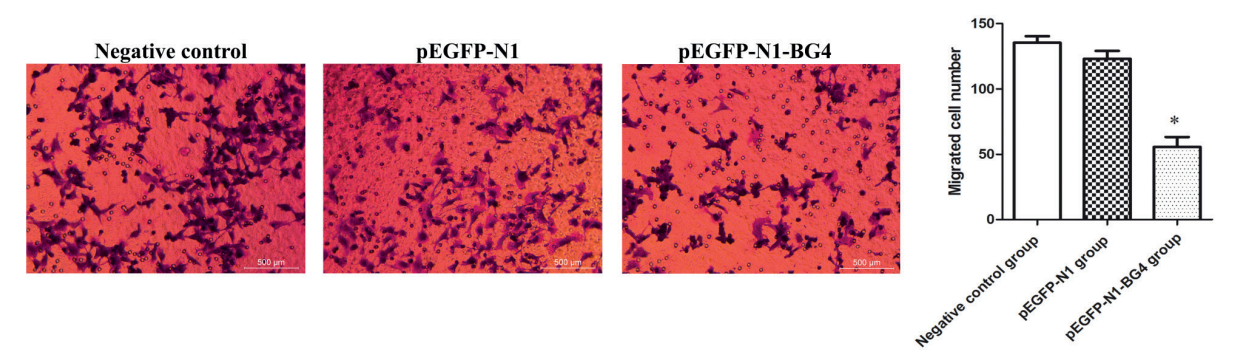


Figure 7. pEGFP-N1-BG4 function on AGS cells assessed *in vitro* by performing transwell migration assays. Representative images of transwell migration assay results and quantification of the inhibitory effects of BG4 on AGS migration (*p<0.01 vs. negative control and pEGFP-N1 group).

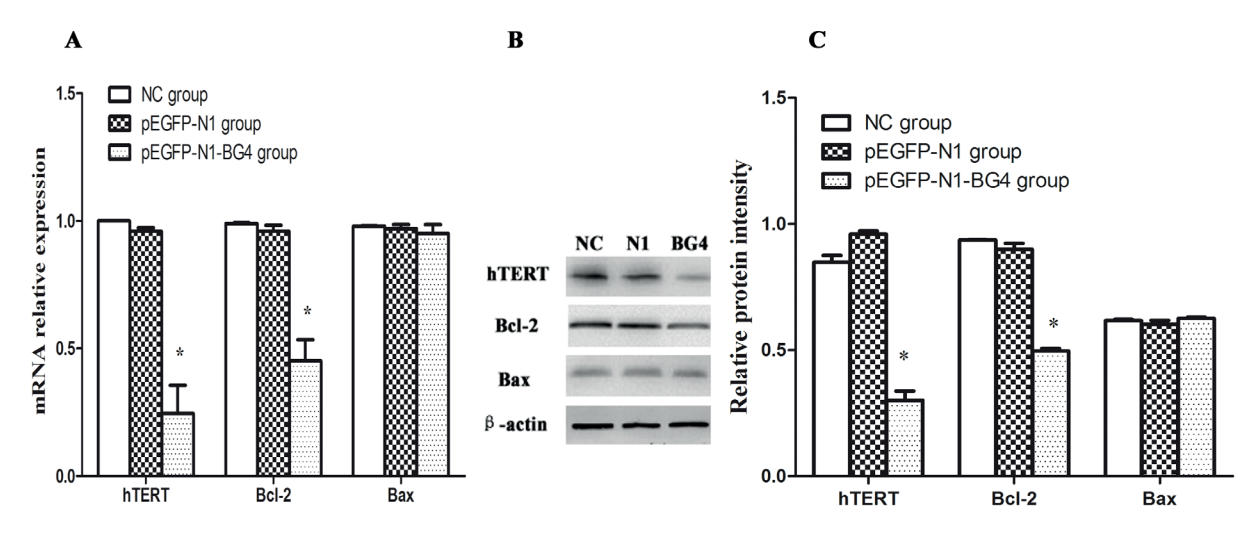


Figure 8. pEGFP-N1-BG4 group regulates the expressions of hTERT and Bcl-2 in AGS cells. **A,** pEGFP-N1-BG4 down-regulates the mRNA expressions of hTERT and Bcl-2 (*p<0.05 vs. NC group and pEGFP-N1 group). **B-C.** pEGFP-N1-BG4 inhibits the protein expressions of hTERT and Bcl-2 (*p<0.05 vs. NC group and pEGFP-N1 group).

the number of AGS cells in S phase sharply declined. We might infer that pEGFP-N1-BG4 could inhibit telomerase activity, disturbed cell cycles and suppressed cell proliferation as well. These changes may be account for the destruction of telomerase's function by G-quadruplex. Both Bax and Bcl-2 are members of Bcl-2 family and regulate cell apoptosis³⁰⁻³². Bax can enhance cell apoptosis, while Bcl-2 plays the opposite function. Bax promotes apoptosis through suppressing the function of Bcl-2 rather than inducing cell apoptosis directly. In AGS cells, both mRNA and protein expressions of Bcl-2 were suppressed by pEGFP-N1-BG4, but no significant changes were identified in Bax. The reason may be that BG4 can stabilize the G-quadruplex structure which is located in the promoter region of Bcl-2, consequently impeding the transcription of Bcl-2 mRNA.

Conclusions

We showed that pEGFP-N1-BG4 inhibited telomerase activity, proliferation and enhanced apoptosis in AGS cells through promoting the formation of G-quadruplex structure. pEGFP-N1-BG4 may serve as a new targeting chemotherapeutic drug in the future. However, there are still some potential limitations of this work. This study was not verified by *in vivo* experiments, and the specific mechanism of BG4 needs further investigation.

Acknowledgements

Research supported by the 1331 Project of Shanxi Province, Health and Family Planning Commission Research Project of Shanxi Province (No.201602032), Changzhi Medical College Science and Technology Launch Fund Project (No.QDZ201502). College Students' Innovation Project (No.D2016004).

Conflict of Interest

The Authors declare that they have no conflict of interest.

References

- Song H, Ekheden IG, Ploner A, Ericsson J, Nyren O, Ye W. Family history of gastric mucosal abnormality and the risk of gastric cancer: A population-based observational study. Int J Epidemiol 2017:
- THEODORATOU E, TIMOFEEVA M, LI X, MENG X, IOANNIDIS J. Nature, nurture, and cancer risks: Genetic and nutritional contributions to cancer. Annu Rev Nutr 2017; 37: 293-320.
- 3) SIEGEL RL, MILLER KD, JEMAL A. Cancer Statistics, 2017. CA Cancer J Clin 2017; 67: 7-30.
- TORRE LA, BRAY F, SIEGEL RL, FERLAY J, LORTET-TIEULENT J, JEMAL A. Global cancer statistics, 2012. CA Cancer J Clin 2015; 65: 87-108.
- CHEN W, ZHENG R, BAADE PD, ZHANG S, ZENG H, BRAY F, JEMAL A, YU XO, HE J. Cancer statistics in China, 2015. CA Cancer J Clin 2016; 66: 115-132.
- SANDHU R, LI B. Telomerase activity is required for the telomere G-overhang structure in Trypanosoma brucei. Sci Rep 2017; 7: 15983.

- Wu Y, BIAN C, ZHEN C, LIU L, LIN Z, NISAR MF, WANG M, BARTSCH JW, HUANG E, JI P, YANG L, YU Y, YANG J, JIANG X, ZHONG JL. Telomerase reverse transcriptase mediates EMT through NF-kappaB signaling in tongue squamous cell carcinoma. Oncotarget 2017; 8: 85492-85503.
- Huang Y, Lin LX, Bi QX, Wang P, Wang XM, Liu J, Wang YT. Effects of hTERT antisense oligodeoxynucleotide on cell apoptosis and expression of hTERT and bcl-2 mRNA in keloid fibroblasts. Eur Rev Med Pharmacol Sci 2017; 21: 1944-1951.
- HANSEL-HERTSCH R, DI ANTONIO M, BALASUBRAMANIAN S. DNA G-quadruplexes in the human genome: Detection, functions and therapeutic potential. Nat Rev Mol Cell Biol 2017; 18: 279-284.
- 10) YADAV K, MEKA P, SADHU S, GUGGILAPU SD, KOVVURI J, KAMAL A, SRINIVAS R, DEVAYANI P, BABU BN, NAGESH N. Telomerase inhibition and human telomeric G-Quadruplex DNA stabilization by a beta-Carboline-Benzimidazole derivative at low concentrations. Biochemistry-Us 2017; 56: 4392-4404.
- 11) SAHA D, SINGH A, HUSSAIN T, SRIVASTAVA V, SENGUPTA S, KAR A, DHAPOLA P, DHOPLE V, UMMANNI R, CHOWDHURY S. Epigenetic suppression of human telomerase (hTERT) is mediated by the metastasis suppressor NME2 in a G-quadruplex-dependent fashion. J Biol Chem 2017; 292: 15205-15215.
- LIN C, YANG D. Human telomeric G-Quadruplex structures and G-Quadruplex-Interactive compounds. Methods Mol Biol 2017; 1587: 171-196.
- 13) SALVATI E, ZIZZA P, RIZZO A, IACHETTINI S, CINGOLANI C, D'ANGELO C, PORRU M, RANDAZZO A, PAGANO B, NOVELLINO E, PISANU ME, STOPPACCIARO A, SPINELLA F, BAGNATO A, GILSON E, LEONETTI C, BIROCCIO A. Evidence for G-quadruplex in the promoter of vegfr-2 and its targeting to inhibit tumor angiogenesis. Nucleic Acids Res 2014; 42: 2945-2957.
- 14) RIGO R, DEAN WL, GRAY RD, CHAIRES JB, SISSI C. Conformational profiling of a G-rich sequence within the c-KIT promoter. Nucleic Acids Res 2017; 45: 13056-13067.
- 15) BISWAS B, KANDPAL M, VIVEKANANDAN P. A G-quadruplex motif in an envelope gene promoter regulates transcription and virion secretion in HBV genotype B. Nucleic Acids Res 2017; 45: 11268-11280.
- 16) LEXA M, STEFLOVA P, MARTINEK T, VORLICKOVA M, VYSKOT B, KEJNOVSKY E. Guanine quadruplexes are formed by specific regions of human transposable elements. BMC Genomics 2014; 15: 1032.
- 17) FLEMING AM, ZHUJ, DING Y, BURROWS CJ. 8-Oxo-7,8-dihydroguanine in the context of a gene promoter G-Quadruplex is an On-Off switch for transcription. ACS Chem Biol 2017; 12: 2417-2426.
- RHODES D, LIPPS HJ. G-quadruplexes and their regulatory roles in biology. Nucleic Acids Res 2015; 43: 8627-8637.
- LAM EY, BERALDI D, TANNAHILL D, BALASUBRAMANIAN S. G-quadruplex structures are stable and detectable in human genomic DNA. Nat Commun 2013; 4: 1796.
- 20) BIFFI G, TANNAHILL D, McCAFFERTY J, BALASUBRAMANIAN S. Quantitative visualization of DNA G-quadruplex

- structures in human cells. Nat Chem 2013; 5: 182-186.
- 21) ZHANG Y, LAN X, WANG S, LI M, LIU Z, SHEN J, SHI S, ZHANG Y, XIE J, CHENG N. [Preparation and identification of DNA G-quadruplex antibody]. Xi Bao Yu Fen Zi Mian Yi Xue Za Zhi 2015; 31: 977-981.
- 22) BIFFI G, TANNAHILL D, MILLER J, HOWAT WJ, BALASUBRA-MANIAN S. Elevated levels of G-quadruplex formation in human stomach and liver cancer tissues. PLoS One 2014; 9: e102711.
- 23) Blasco MA. Telomeres and human disease: Ageing, cancer and beyond. Nat Rev Genet 2005; 6: 611-622.
- 24) DE LANGE T. Protection of mammalian telomeres. Oncogene 2002; 21: 532-540.
- 25) LIN TT, LETSOLO BT, JONES RE, ROWSON J, PRATT G, HEWAMANA S, FEGAN C, PEPPER C, BAIRD DM. Telomere dysfunction and fusion during the progression of chronic lymphocytic leukemia: evidence for a telomere crisis. Blood 2010; 116: 1899-1907.
- 26) Colla S, Ong DS, Ogoti Y, Marchesini M, Mistry NA, Clise-Dwyer K, Ang SA, Storti P, Viale A, Giuliani N, Ruisaard K, Ganan GI, Bristow CA, Estecio M, Weksberg DC, Ho YW, Hu B, Genovese G, Pettazzoni P, Multani AS, Jiang S, Hua S, Ryan MC, Carugo A, Nezi L, Wei Y, Yang H, D'Anca M, Zhang L, Gaddis S, Gong T, Horner JW, Heffernan TP, Jones P, Cooper LJ, Liang H, Kantarjian H, Wang YA, Chin L, Bueso-Ramos C, Garcia-Manero G, DePinho RA. Telomere dysfunction drives aberrant hematopoietic differentiation and myelodysplastic syndrome. Cancer Cell 2015; 27: 644-657.
- 27) CLYNES D, JELINSKA C, XELLA B, AYYUB H, SCOTT C, MITSON M, TAYLOR S, HIGGS DR, GIBBONS RJ. Suppression of the alternative lengthening of telomere pathway by the chromatin remodelling factor ATRX. Nat Commun 2015; 6: 7538.
- 28) Das A, Chatterjee S, Suresh KG. Targeting human telomeric G-quadruplex DNA with antitumour natural alkaloid aristololactam-beta-D-glucoside and its comparison with daunomycin. J Mol Recognit 2017; 30:
- 29) ZHANG YO, ZHANG YH, XIE J, LI MN, LIU ZR, SHEN JY, SHI SS, LAN XY, WANG S, CHENG NL. TMPyP4-regulated cell proliferation and apoptosis through the Wnt/ beta-catenin signaling pathway in SW480 cells. J Recept Signal Transduct Res 2016; 36: 167-172.
- 30) TEYMOURNEJAD O, MOBAREZ AM, HASSAN ZM, TALE-BI BAA. Binding of the Helicobacter pylori OipA causes apoptosis of host cells via modulation of Bax/Bcl-2 levels. Sci Rep 2017; 7: 8036.
- 31) Li H, Lv B, Kong L, Xia J, Zhu M, Hu L, Zhen D, Wu Y, Jia X, Zhu S, Cui H. Nova1 mediates resistance of rat pheochromocytoma cells to hypoxia-induced apoptosis via the Bax/Bcl-2/caspase-3 pathway. Int J Mol Med 2017; 40: 1125-1133.
- 32) SKALA E, SITAREK P, TOMA M, SZEMRAJ J, RADEK M, NIE-BOROWSKA-SKORSKA M, SKORSKI T, WYSOKINSKA H, SLIWINSKI T. Inhibition of human glioma cell proliferation by altered Bax/Bcl-2-p53 expression and apoptosis induction by Rhaponticum carthamoides extracts from transformed and normal roots. J Pharm Pharmacol 2016; 68: 1454-1464.